Chinese Chemical Letters 34 (2023) 108183

Contents lists available at ScienceDirect

Chinese Chemical Letters

journal homepage: www.elsevier.com/locate/cclet

Construction of 3,9-diazatetraasteranes and 3,9-diazatetracyclododecanes by photocycloaddition reaction of 1,4-dihydropyridines: Experimental and theoretical investigation

Runzhi Sun[a], Xiuqing Song[b], Shijie Wang[a], Xiaokun Zhang[a], Hong Yan[a,*], Yeming Wang[c,*]

[a] Faculty of Environment and Life, Beijing University of Technology, Beijing 100124, China
[b] Large-scale Instruments and Equipments Sharing Platform, Beijing University of Technology, Beijing 100124, China
[c] Beijing Tide Pharmaceutical Co., Ltd., Beijing 100176, China

ARTICLE INFO

Article history:
Received 14 November 2022
Revised 11 January 2023
Accepted 29 January 2023
Available online 3 February 2023

Keywords:
1,4-Dihydropyridine
Photocycloaddition
Theoretical investigation
3,9-Diazatetracyclododecanes

ABSTRACT

A photocycloaddition reaction of ethyl 1,4-diaryl-1,4-dihydropyridine-3-carboxylate for the construction of 3,9-diazatetraasteranes ($\mathbf{P_1}$) and 3,9-diazatetracyclododecanes ($\mathbf{P_2}$) is reported for the first time. The types of reaction product clearly differ with solvent, regardless of the irradiation wavelength. The difference in $\mathbf{P_1}$ and $\mathbf{P_2}$ lies in the second step of the intramolecular [2 + 2] photocyclization. In order to further investigate this phenomenon and gain a deeper understanding of the photochemical behavior of 1,4-dihydropyridines, DFT and TDDFT theoretical calculations are performed. The results provide a good explanation for the formation of 3,9-diazatetraasteranes and 3,9-diazatetracyclododecanes.

Cycloaddition reactions are a universal and straightforward pathway to carbocyclic or heterocarbocyclic organic compounds in which two or more bonds may be formed in a single operation [1]. The photochemical [2 + 2] cycloaddition reaction is the most frequently used cycloaddition reaction to access carbocyclic products with structural moieties of cyclobutane rings [2–12]. Carbocyclic products incorporating fused cyclobutane rings, such as cubane, homocubane, tetraastarane, and pentacycloundecane, continue to attract attention in drug discovery for their higher conformational rigidity and lipophilicity [13–16]. The cyclobutane ring has multiple sp^3 scaffolds in the three-dimensional structure, which not only provide a unique chemical space, but are also correlated to improve the pharmacokinetic properties and toxicological benefits [17]. The photochemical [2 + 2] cycloaddition reaction involve two olefins as substrates, one of which is required to be excited by ultraviolet light. There are a wide variety of olefins, such as thymoquinone, α-truxillic acid, enone [18–20]. Typical olefins are the (+)-carvone for carvone camphor, the *endo*-dimer of 2-bromocyclopentadienone for the key intermediates of the cubane ring system, the Diels-Alder adduct of *p*-bensoquinone and cyclopentadiene for pentacycloundecanes (Cookson's diketone), and the 1,4-dihydrophthalic anhydride for tetraastarane derivatives, and so on [21–22].

As an important and common structural unit, 1,4-dihydropyridines (1,4-DHPs) are commonly used clinically as calcium antagonists and antimicrobials for the treatment of cardiovascular disease [23–29]. Similar to 1,4-dihydrophthalic anhydride, the two double bonds in 1,4-DHPs enable them to undergo [2 + 2] photocycloaddition to provide diazatetraasteranes [30–32]. Historically, the first [2 + 2] photocycloadditions of 1,4-DHPs were found in the chemical literature, as reported by Eisner in 1970. The [2 + 2] photocyclization of 3,5-dicarbonyl-1,4-DHPs had given 3,9-diazatetraasteranes with a medium-pressure mercury lamp (MPM) as the light source (Scheme 1a) [33], while the [2 + 2] photocyclization of 3-carbonyl-1,4-DHPs had given 3,9-diazatetraasteranes under a high-pressure mercury lamp (Scheme 1b) [31,34-35]. The regioselective [2 + 2] photocycloaddition of 3,5-dicarbonyl-1,4-dihydropyridines had given 3,6-diazatetraasterane *via* a covalent link in a head-to-head manner by the phthaloyl group (Scheme 1c) [36]. The 3,9-diazatetraasteranes, so as it is the structure analogue of 3,9-dioxotetraasteranes, shows good pharmacological activity, with HIV-1 protease inhibitory activity for C_2 symmetry, and anti-tumor activity by inhibiting epidermal growth factor receptor (EGFR) and so on [37–40]. Therefore, the study of the synthesis and pharmacological activity of 3,9-diazatetraasteranes and their analogs have attracted extensive attention in recent years [41–44].

To continue research into the [2 + 2] photocycloaddition of 1,4-DHPs, UV LED lamps were used to replace the traditional

* Corresponding authors.
E-mail addresses: hongyan@bjut.edu.cn (H. Yan), yemingwang@126.com (Y. Wang).

https://doi.org/10.1016/j.cclet.2023.108183
1001-8417/

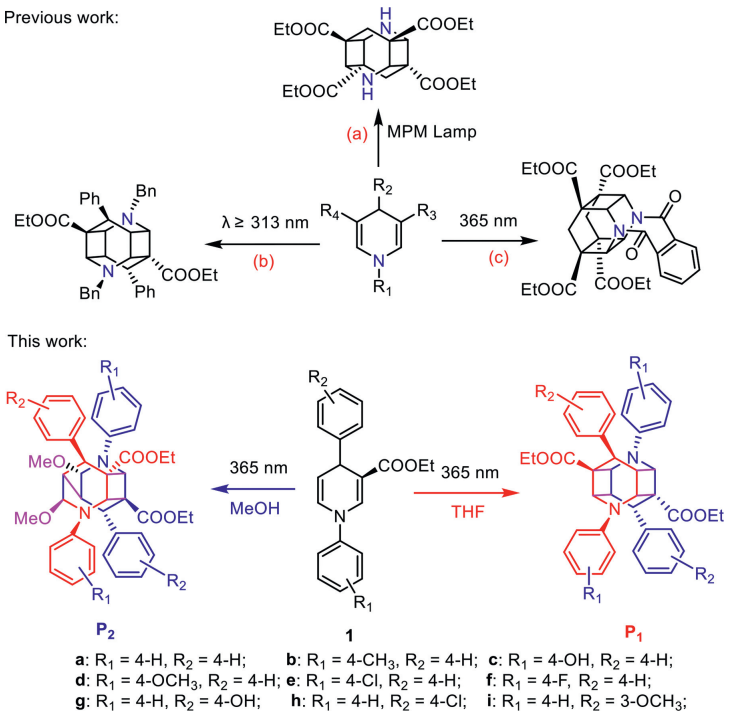

Scheme 1. [2 + 2] Photocycloadditions of 1,4-DHPs (**1**).

mercury lamps in order to improve the synthetic efficiency of 3,9-diazatetraasteranes with ethyl 3-carboxylate-1,4-DHPs (**1**) as olefins. When using **1** as the substrate, the reaction products were found to differ clearly with solvent, regardless of the wavelength of the LED lamp. The 3,9-diazatetraasteranes ($\mathbf{P_1}$) were obtained in tetrahydrofuran, while $\mathbf{P_1}$ and unexpected 3,9-diazatetracyclododecanes ($\mathbf{P_2}$) were observed in methanol. (Scheme 1). In order to elucidate this phenomenon, density-functional theory (DFT) and time-dependent DFT (TDDFT) theoretical calculations were performed.

Initially, our idea was to improve the synthetic efficiency of 3,9-diazatetraasteranes ($\mathbf{P_1}$) by using UV LED lamps instead of traditional mercury lamps. To optimize the reaction conditions, the factors such as the light source, irradiation wavelength, solvent, atmosphere and substituent of 1,4-DHPs (**1**), were systematically screened. The photocycloaddition of **1a** was selected as the model compound (Table 1). It was worth mentioning that there was more than one product, with both $\mathbf{P_1}$ and unexpected $\mathbf{P_2}$ produced in MeOH solvent. The yields of the products clearly differed with solvent, regardless of wavelength. The synthetic efficiency of 3,9-diazatetraasterane ($\mathbf{P_1}$) was significantly improved, and the reaction time decreased from 8 weeks, as reported in the literature, to about 20 h.

Table 1
Yields of $\mathbf{P_{1a}}$ and $\mathbf{P_{2a}}$ under different reaction conditions.

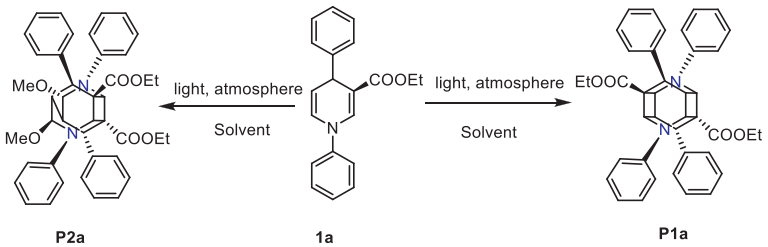

Entry	Solvents	Atmosphere	HPM 500W		365 nm (LED)		395 nm (LED)	
			$\mathbf{P_{1a}}$[b]	$\mathbf{P_{2a}}$[c]	$\mathbf{P_{1a}}$	$\mathbf{P_{2a}}$	$\mathbf{P_{1a}}$	$\mathbf{P_{2a}}$
1	THF	N_2	25	0	56	0	35	0
2	THF	air	10	0	20	0	15	0
3	Benzene	N_2	13	0	35	0	23	0
4	MeCN	N_2	10	0	28	0	20	0
5	MeOH	N_2	Trace	23	12	52	<10	37
6	MeOH	air	<10	10	10	14	<10	<10
7	MeOH/THF = 1:1	N_2	10	15	18	43	12	28

[a] Reaction conditions: **1a** (3 mmol, 0.92 g), solution concentration 0.2 mol/L, at room temperature, the complete conversion of **1a** (detected by thin layer chromatography [TLC]) required about 20 h.
[b] Isolated yields obtained *via* column chromatography (EA/PE = 1/5, v/v).
[c] Isolated yields obtained *via* recrystallization in MeOH/dichloromethane (DCM).

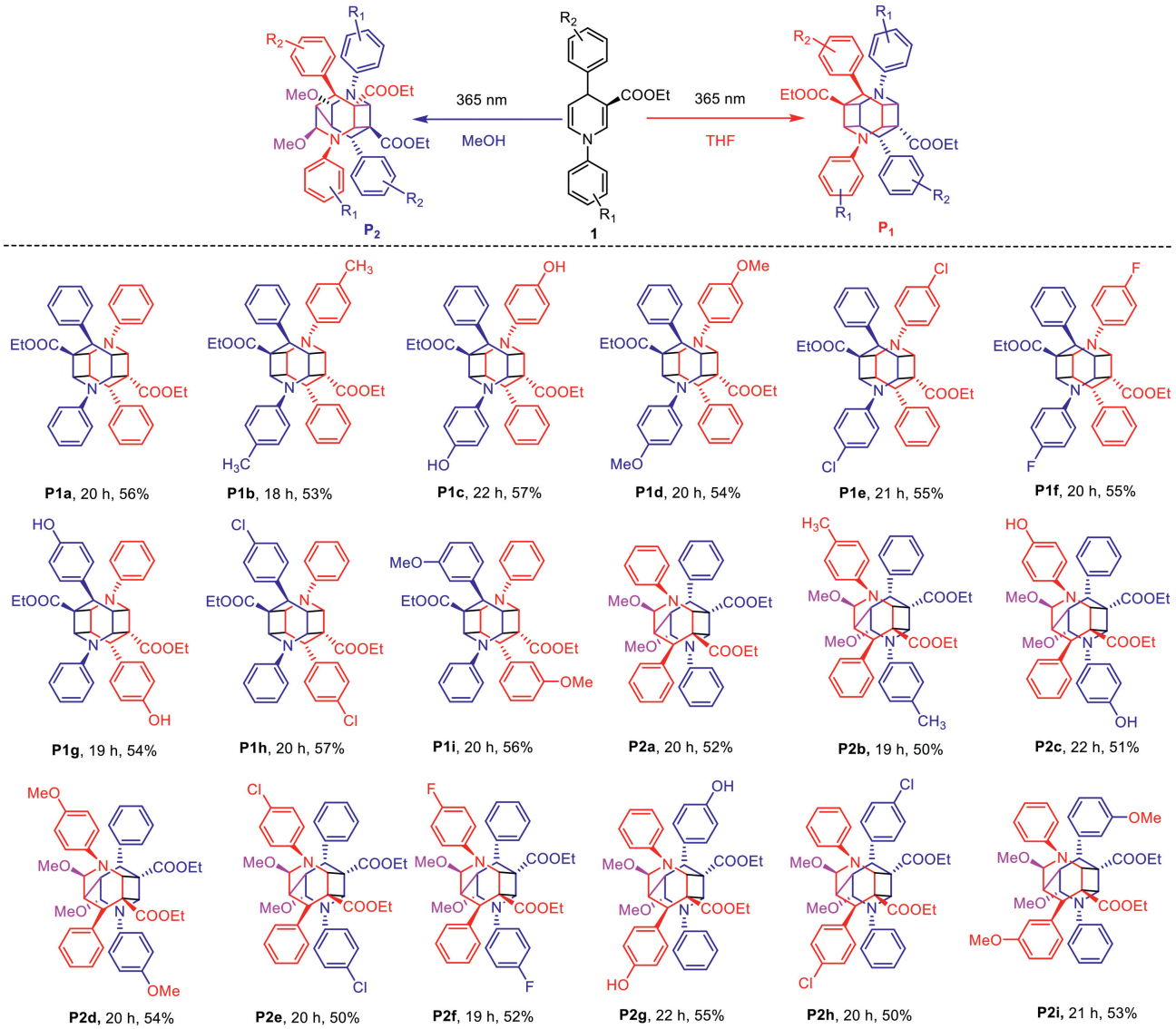

Scheme 2. Structures and yields of 3,9-diazatetraasteranes ($\mathbf{P_1}$) and 3,9-diazatetracyclododecanes ($\mathbf{P_2}$).

As shown in Table 1, whether it was the formation of $\mathbf{P_{1a}}$ or $\mathbf{P_{2a}}$, the yields under an N_2 atmosphere were higher than those without it. The reason was that oxygen in the air could generate the excited state singlet oxygen ($^1O_2$) to reduce the yield by combining with carbon radicals. The irradiation wavelengths did not affect the type of product, but only affected the yield of product.

Under irradiation at 365 nm LED lamp under an N_2 atmosphere, $\mathbf{P_{1a}}$ was obtained in 56% yield in THF, while $\mathbf{P_{2a}}$ was obtained in 52% yield with 12% of $\mathbf{P_{1a}}$ in MeOH (Table 1, entries 1 and 5). The generalizability of the different substituted 1,4-diaryl-3-carboxylate-1,4-DHPs (**1**) was investigated (Scheme 2). The yields of $\mathbf{P_1}$ were 53%–57%, and those of $\mathbf{P_2}$ were about 50%–53%. The substituents on the 1,4-DHPs had little effect on the yields of $\mathbf{P_1}$ and $\mathbf{P_2}$. The structures of all synthesized $\mathbf{P_1}$ and $\mathbf{P_2}$ were confirmed by NMR and HRMS, especially the structures of $\mathbf{P_{1d}}$ & $\mathbf{P_{2a}}$ were confirmed by single crystal X-ray diffraction (Scheme 2, Fig. 1).

Based on the [2 + 2] cycloaddition of α, β-enone and alkene derivatives and the mechanism of the 3,5-disubtitued-1,4-DHPs [45–48], the possible mechanisms for the formation of $\mathbf{P_1}$ and $\mathbf{P_2}$ were proposed, as shown in Scheme 3. Considering the substituents had little effect on this reaction, the mechanism was discussed using **1a** as a model compound. The formation mechanism

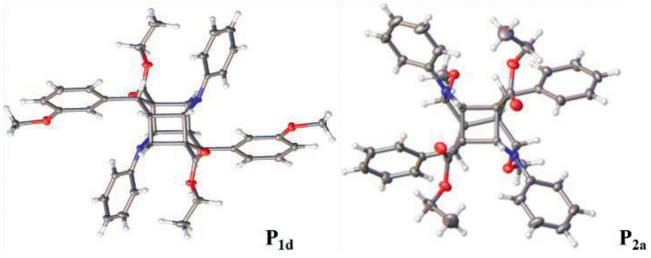

Fig. 1. Structures of $\mathbf{P_{1d}}$ and $\mathbf{P_{2a}}$ obtained by X-ray single-crystal diffraction.

of $\mathbf{P_{1a}}$ was the [2 + 2] photocycloaddition of 1,4-DHP (**1**), which may presumably be divided into two steps. The first step was the intermolecular [2 + 2] photocycloaddition. The second step was the intramolecular [2 + 2] photocycloaddition of the *syn*-dimer **2a** to form $\mathbf{P_{1a}}$ (Path 1a). The formation mechanism of $\mathbf{P_{2a}}$ was the [2 + 2] photocycloaddition of 1,4-DHP (**1**), similar that of $\mathbf{P_{1a}}$, containing an intermolecular [2 + 2] and a half intramolecular [2 + 2] photocyclization. The difference was that in the intramolecular [2 + 2] photocyclization of **2a**, the first σ-bond was formed

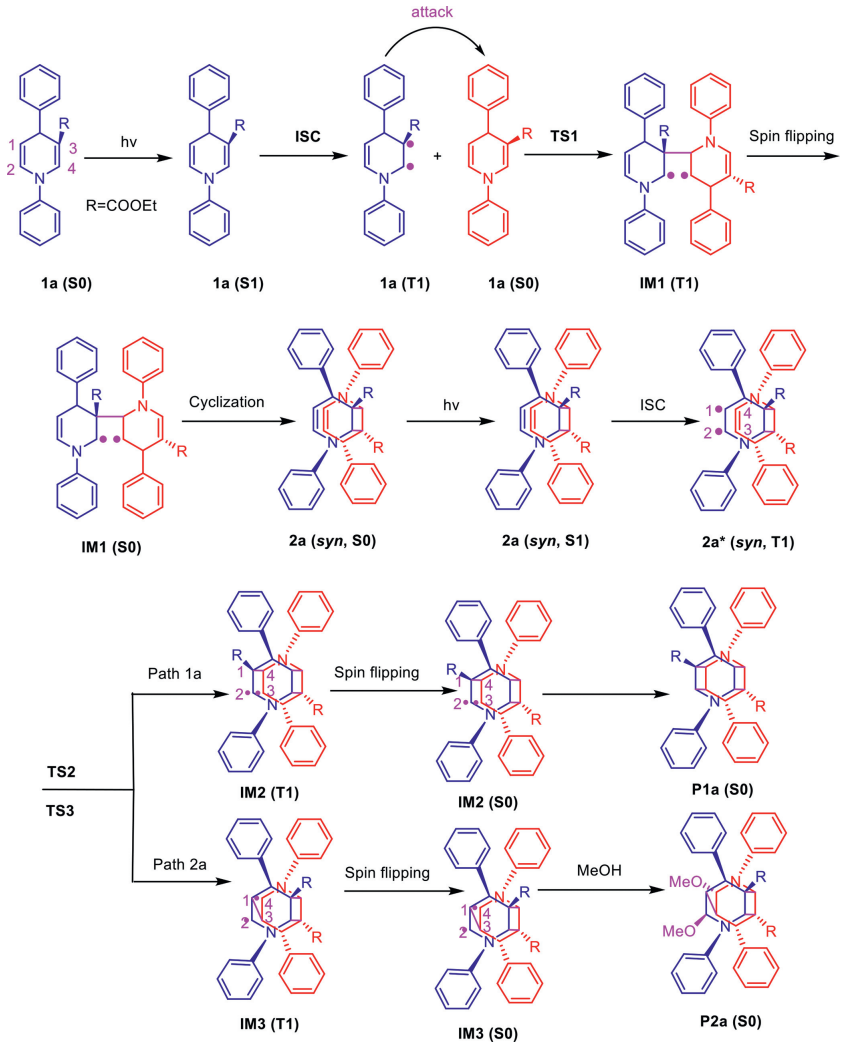

Scheme 3. Proposed formation mechanism of 3,9-diazatetraasteranes ($\mathbf{P_1}$) and 3,9-diazatetracyclododecanes ($\mathbf{P_2}$).

at different sites to that of $\mathbf{P_{1a}}$. The two carbon radicals at the cross position combined with each other, resulting in the inability to form a second σ-bond, but instead the solvent became involved, and the carbon radicals combined with the methoxy radicals provided by the MeOH, to form two C–O σ-bonds in $\mathbf{P_{2a}}$.

At the PCM/B3LYP/def2-TZVP//B3LYP/6–31 g(d) level, DFT/TDDFT calculations were carried out to investigate the favorable [2 + 2] photocycloaddition pathways of the 1,4-DHPs (**1**). The calculated free energies of the formation pathways in MeOH were discussed, and the reactive sites of **2a** ($\mathbf{T_1}$) was qualitatively analyzed using the Fukui function. The formation mechanisms of $\mathbf{P_1}$ and $\mathbf{P_2}$ were the [2 + 2] photocycloaddition of 1,4-DHPs (**1**), which could be divided into two steps. The first steps were the intermolecular [2 + 2] photocycloaddition to form a *syn*-dimer **2a**. The second steps were the intramolecular [2 + 2] photocycloaddition of the *syn*-dimer **2a** in both cases, with the difference being that $\mathbf{P_2}$ in a half intramolecular [2 + 2] photocyclization involved MeOH (Path 1a and Path 2a).

According to theoretical research on the [2 + 2] photocycloaddition mechanism of the 1,4-DHPs, the formation of *syn*-dimer **2a** was similar to the first step in previous reports [26]. Therefore, the calculation analysis focused on the second steps in order to elucidate the differences in the formation of $\mathbf{P_1}$ and $\mathbf{P_2}$. In the following discussion, the most stable conformation of **1a** was used, and its Gibbs free energy was used as the energy reference point.

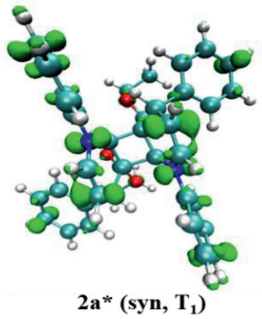

Fig. 2. Fukui function f(0) surface atom in **2a*** (***syn*, $\mathbf{T_1}$**) (isovalue = 0.002).

First, the reactive sites of **2a*** (***syn*, $\mathbf{T_1}$**) were qualitatively analyzed using the Fukui function, and the isosurface graphs of **2a*** (***syn*, $\mathbf{T_1}$**) were displayed in Fig. 2. The isosurface graphs of **2a*** (***syn*, $\mathbf{T_1}$**) showed that unpaired electrons were mainly distributed on the C1 and C3 atoms, with a few electrons distributed on the C2 and C4 atoms. The C1 and C3 atoms were more likely to be the sites of photoreaction with the highest reactivity, which was consistent with the experimental results that $\mathbf{P_{2a}}$ formed the C–C single bond at the cross position first.

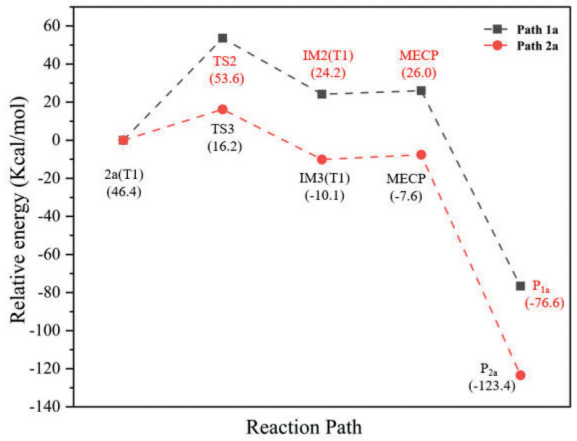

Fig. 3. Energy profile of Path 1a and Path 2a and their relative Gibbs free energies (kcal/mol).

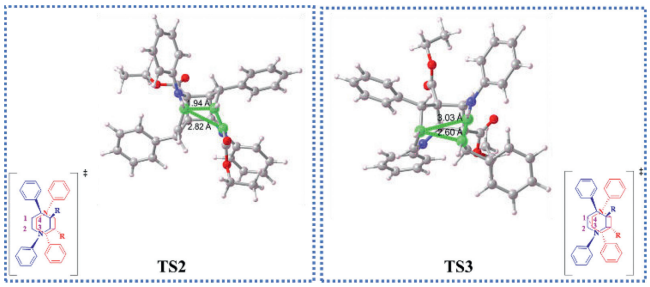

Fig. 4. Optimized structures and significant bond distances of transition states (TS2 and TS3).

Second, the energy profile of Path 1a and Path 2a in MeOH and their relative Gibbs free energy were calculated (Fig. 3). The energy barrier of the **IM2** ($\mathbf{T_1}$) formation through the transition state **TS2** (Path 1a) was 53.6 kcal/mol, and that of the **IM3** ($\mathbf{T_1}$) formation through the transition state **TS3** (Path 2a) was only 16.2 kcal/mol. **IM3** ($\mathbf{T_1}$) was more favorable to form than **IM2** ($\mathbf{T_1}$). In the conversion of **IM2** ($\mathbf{T_1}$) and **IM3** ($\mathbf{T_1}$) to **IM2** ($\mathbf{S_0}$) and **IM3** ($\mathbf{S_0}$), spin-flipping was required, and the minimal energy crossing point (**MECP**) between $\mathbf{T_1}/\mathbf{S_0}$ was successfully localized. The free energies were 1.8 kcal/mol and 2.5 kcal/mol, respectively, so the two spin-flipping processes were readily occurred. In the conversion of **IM2** ($\mathbf{T_1}$) to $\mathbf{P_{1a}}$, the second σ-bond formed between the C2 and C3 radicals (ring-closure) was proven to be barrierless [26]. In the conversion of **IM3** ($\mathbf{T_1}$) to $\mathbf{P_{2a}}$, the form C–O σ-bond involving C2 or C4 with methoxy radicals was speculated to suggest the possible existence of another transition state, but attempted to locate the transition site failed several times. This was finally proven to be a barrierless process by the means of relaxed scanning of the bond distance (C2-O3), wherein energy decreased continuously with the shortening of the bond distance (Fig. 5). Therefore, the rate-determining steps of Path 1a and Path 2a were the first σ-bond formation. The overall energy barrier was 53.6 kcal/mol and 16.2 kcal/mol, respectively. The Gibbs free energy of $\mathbf{P_{1a}}$ and $\mathbf{P_{2a}}$ was −76.6 kcal/mol and −123.4 kcal/mol, respectively. This suggests that Path 2a was the dominant pathway in both thermodynamically and kinetically. This was consistent with the experimental results showing that the yield of $\mathbf{P_2}$ was always much greater than that of $\mathbf{P_1}$ in MeOH.

In conclusion, under irradiation at 365 nm LED lamp in an N_2 atmosphere, it was shown that the photocycloaddition reaction of ethyl 1,4-diaryl-1,4-dihydropyridine-3-carboxylate reaction could tolerate different substituents, with yields of $\mathbf{P_1}$ of about 55% in

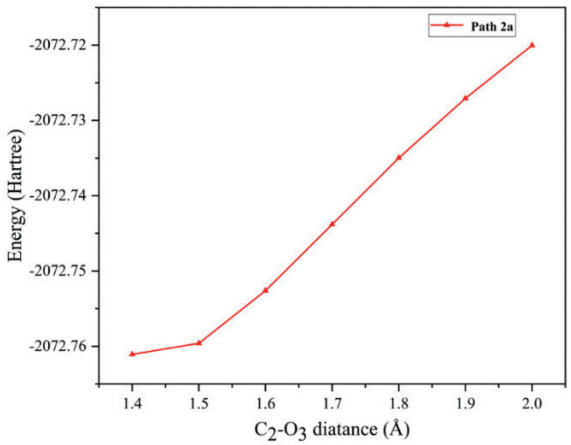

Fig. 5. Relaxed scanning curves for the combination of C_2 and methoxy radical.

THF, and that yields of $\mathbf{P_2}$ of about 50% in methanol. The formation mechanism of $\mathbf{P_1}$ and $\mathbf{P_2}$ was speculated to occur in two steps; the first step was the intermolecular [2 + 2] photocycloaddition which formed the *syn*-dimer **2a**, the second step was the intramolecular [2 + 2] photocycloaddition of the *syn*-dimer **2a** to form $\mathbf{P_1}$, or a half intramolecular [2 + 2] photocyclization involving MeOH solvent to form $\mathbf{P_2}$. The rate-determining steps in the process of the *syn*-dimer **2** to $\mathbf{P_1}$ and $\mathbf{P_2}$ (Path 1a and Path 2a) were all the first σ-bond formation in **IM2** ($\mathbf{T_1}$) and **IM3** ($\mathbf{T_1}$). The calculated values of the energy barrier and the Gibbs free energy also suggested that Path 2a was the dominant pathway both thermodynamically and kinetically, meaning that $\mathbf{P_{2a}}$ was the dominant product, and it was consistent with the experimental results.

Declaration of competing interest

The authors declare that they have no known competing financial interests or personal relationships that could have appeared to influence the work reported in this paper.

Acknowledgment

This work was supported by the Beijing Natural Science Foundation (No. 2192004).

References

[1] L.R. Domingo, S.R. Emamian, Tetrahedron 70 (2014) 1267–1273.
[2] S. Poplata, A. Tröster, Y. Zou, T. Bach, Chem. Rev. 116 (2016) 9748–9815.
[3] V.M. Dembitsky, J. Nat. Med. 62 (2008) 1–33.
[4] S. Piao, Y. Song, W. Jiao, et al., Org. Lett. 15 (2013) 3526–3529.
[5] R. Medishetty, A. Husain, Z. Bai, et al., Angew. Chem. Int. Ed. 126 (2014) 6017–6021.
[6] A.E. Hurtley, Z. Lu, T.P. Yoon, Angew. Chem. Int. Ed. 126 (2014) 9137–9140.
[7] C. García-Morales, B. Ranieri, I. Escofet, et al., J. Am. Chem. Soc. 139 (2017) 13628–13631.
[8] M.A. Ischay, Z. Lu, T.P. Yoon, J. Am. Chem. Soc. 132 (2010) 8572–8574.
[9] D. Yang, Q. Yan, E. Zhu, J. Lv, W.M. He, Chin. Chem. Lett. 33 (2022) 1798–1816.
[10] S. He, X. Chen, F. Zeng, et al., Chin. Chem. Lett. 31 (2020) 1863–1867.
[11] W. He, L. Gao, X. Chen, et al., Chin. Chem. Lett. 31 (2020) 1895–1898.
[12] Z. Gan, G. Li, X. Yang, et al., Sci. China Chem. 63 (2020) 1652–1658.
[13] A. Sergeiko, V.V. Poroikov, L.O. Hanus, V.M. Dembitsky, Open. Med. Chem. J. 2 (2008) 26–37.
[14] Y. Fan, X. Gao, J. Yue, Sci. China Chem. 59 (2016) 1126–1141.
[15] B. Zhang, J. Chen, Chin. J. Org. Chem. 42 (2022) 3429–3430.
[16] W. Zhou, Y. Jiang, L. Chen, K. Liu, D. Yu, Chin. J. Org. Chem. 40 (2020) 3697–3713.
[17] J.M. Anderson, N.D. Measom, J.A. Murphy, D.L. Poole, Angew. Chem. Int. Ed. 60 (2021) 24754–24769.
[18] J. Bertram, R. Kürsten, J. Prakt. Chem. 51 (1895) 316–325.
[19] C.N. Riiber, Ber. Dtsch. Chem. Ges. 35 (1902) 2908–2909.
[20] G. Ciamician, P. Silber, Ber. Dtsch. Chem. Ges. 35 (1902) 1992–2000.
[21] G. Ciamician, P. Silber, Ber. Dtsch. Chem. Ges. 41 (1908) 1071–1080.

[22] G. Büchi, I. Goldman, J. Am. Chem. Soc. 79 (1957) 4741–4748.
[23] S. Goldmann, J. Stoltefuss, Angew. Chem. Int. Ed. 30 (1991) 1559–1578.
[24] D.J. Triggle, D.A. Langs, R.A. Janis, Med. Res. Rev. 9 (1989) 123–180.
[25] F. Bossert, W. Vater, Med. Res. Rev. 9 (1989) 291–324.
[26] Q. Fan, H. Tan, P. Li, H. Yan, New J. Chem. 42 (2018) 16795–16805.
[27] M.S. Saddala, R. Kandimalla, J.A. Pradeepkiran, S.S. Bhashyam, U.R. Asupatri, Sci. Rep. 7 (2017) 45211.
[28] I. Drapak, L. Perekhoda, T. Tsapko, N. Berezniakova, Y. Tsapko, J. Heterocycl. Chem. 54 (2017) 2117–2128.
[29] M. Zhang, H. Lan, N. Li, et al., J. Org. Chem. 85 (2020) 8279–8286.
[30] C. Coburger, J. Wollmann, M. Krug, et al., Bioorgan. Med. Chem. 18 (2010) 4983–4990.
[31] A. Hilgeroth, M. Wiese, A. Billich, J. Med. Chem. 42 (1999) 4729–4732.
[32] Y. Liu, H. Tan, H. Yan, X. Song, Chem. Biol. Drug. Des. 82 (2013) 567–578.
[33] U. Eisner, J.R. Williams, B.W. Matthews, H. Ziffer, Tetrahedron 26 (1970) 899–909.
[34] A. Hilgeroth, H. Lilie, Eur. J. Med. Chem. 38 (2003) 495–499.
[35] M. Richter, J. Molnár, A. Hilgeroth, J. Med. Chem. 49 (2006) 2838–2840.
[36] H. Tan, Z. Zhao, Z. Ma, H. Yan, Tetrahedron 74 (2018) 529–534.
[37] A. Hilgeroth, U. Baumeister, F.W. Heinemann, Eur. J. Med. Chem. 2000 (2000) 245–249.
[38] A. Hilgeroth, J. Molnár, E. De Clercq, Angew. Chem. Int. Ed. 41 (2002) 3623–3625.
[39] A. Hilgeroth, A. Billich, Arch. Pharm. 332 (1999) 380–384.
[40] L. Mao, N. Tian, C. Wei, H. Wang, H. Yan, Russ. J. Gen. Chem. 92 (2022) 446–456.
[41] P. Chen, H. Wang, M. Li, et al., Dis. Markers. 2020 (2020) 5068067.
[42] Q. Fan, L. Zhu, H. Ren, H. Lin, G. Wu, Chem. Phys. Lett. 771 (2021) 2207–2213.
[43] H. Xin, X. Zhu, H. Yan, X. Song, Tetrahedron Lett. 54 (2013) 3325–3328.
[44] Q. Song, H. Wang, H. Yan, C. Ni, R. Zhong, J. Mol. Struct. 1006 (2011) 489–493.
[45] G.M.J. Schmidt, Pure. Appl. Chem. 27 (1971) 647–678.
[46] E. García-Expósito, M.J. Bearpark, R.M. Ortuño, M.A. Robb, V. Branchadell, J. Org. Chem. 67 (2002) 6070–6077.
[47] P. Jaque, A. Toro-Labbé, P. Geerlings, F.D. Proft, J. Phys. Chem. A 113 (2009) 332–344.
[48] S. Wilsey, L. González, M.A. Robb, K.N. Houk, J. Am. Chem. Soc. 122 (2000) 5866–5876.